Vibrationally autoionizing Rydberg clusters: Spectroscopy and dynamics of pyrazine-Ar and -Xe clusters

doi: 10.1063/1.1315359

Vibrationally autoionizing Rydberg clusters: Spectroscopy and dynamics of pyrazine–Ar and –Xe clusters

Asuka Fujii,[a] Yutaka Kitamura, and Naohiko Mikami[a]
Department of Chemistry, Graduate School of Science, Tohoku University, Sendai 980-8578, Japan

(Received 24 April 2000; accepted 15 August 2000)

Vibrational autoionization spectra of high Rydberg states of pyrazine–Ar and –Xe van der Waals clusters were observed by two-color double resonance spectroscopy. Two Rydberg series converging to the same ionization threshold appeared in the spectra of both the clusters, while only one Rydberg series was seen in bare pyrazine. One of the series of the clusters was assigned to be of ''gerade,'' which is the same Rydberg series as that found in bare pyrazine. The other series of the clusters was assigned to an ''ungerade'' series, suggesting that the symmetry breakdown of the ion core is induced by the cluster formation. For both the Rydberg series, apparently very small quantum defects were involved, and the ''gerade'' and ''ungerade'' series were tentatively assigned to the *d* (or *s*) and *f* Rydberg series, respectively. In comparison with the bare molecule, the quantum defects of the clusters exhibited slight shifts to the negative direction, indicating the decrease of the binding energy of the Rydberg electron. The vibrational autoionization efficiency does not change upon the cluster formation, even above the dissociation threshold of the van der Waals bond. This fact indicates that the vibrational autoionization rate is much faster than the vibrational predissociation rate. © *2000 American Institute of Physics.* [S0021-9606(00)00842-4]

I. INTRODUCTION

Observations of high Rydberg states near the converging limit have been very scarce for molecular clusters.[1–5] Because the orbital radius of the Rydberg electron is much larger than the size of the ion core, the intermolecular potential is reasonably predicted to be almost the same as that of bare cluster cation. However, the quasi-Coulomb field of the ion core would be perturbed by the cluster formation, and the energy shift of the Rydberg states is expected to reflect such a perturbation to the field from the solvent molecules. Such situation is quite different from that in low lying Rydberg states (principal quantum number, *n*, is lower than 10 or so), which have been so far studied in Hg,[6] NO,[7] I_2,[8] ABCO,[9] DABCO,[10] and hexamethylenetetramine[11] with rare gas solvents. In low Rydberg clusters, the intermolecular distance is close to the Rydberg orbital radius, and it has been shown that the interference from the Rydberg electron plays an important role in the intermolecular potentials.

Dynamics of high Rydberg clusters is also of particular importance. High Rydberg states can lie above the first ionization threshold (IP_0) with the vibrational excitation of the ion core. Such states (so-called superexcited states) decay through the energy transfer from the ion core to the Rydberg electron, i.e., vibrational autoionization.[12] Competition between the autoionization and electronic predissociation has been the subject of much interest in the dynamics of superexcited states.[12–14] In the case of Rydberg clusters, vibrational predissociation (breaking of the intermolecular bond) can also be a decay channel of the vibrational energy of the ion core. Though there has been no study on the competition between the vibrational autoionization and vibrational predissociation, such competition should be important in the dynamics of Rydberg states in condensed phases.

Molecular clusters produced in a supersonic jet expansion have been extensively studied as a microscopic model of condensed phases, and details of solvation effects have been successfully elucidated by using simplified cluster systems.[15] However, most of the cluster studies so far focus on the electronic ground and low lying excited states, and solvation effects in highly excited electronic states are still an unresolved problem. It has not yet been known whether vibrational autoionization can occur in condensed phases. Experimental studies in clusters are expected to give an important suggestion for this unresolved question. In addition, the relation between Rydberg states in a bulk system and geminate pair which is produced upon ionization in the material has been discussed.[16] Therefore, Rydberg clusters should have the rich implication to understand the complex mechanism of ionization in the condensed phase.

In this paper, we report the study on spectroscopy and dynamics of superexcited Rydberg states of pyrazine–Ar and –Xe clusters. Pyrazine is one of rare polyatomic molecules of which high Rydberg states have been well studied. Goto *et al.* applied two-color double resonance spectroscopy to bare pyrazine in a supersonic jet.[17] They pumped various vibrational levels of the $S_1(n,\pi^*)$ state, and probed transitions from S_1 to high Rydberg states above IP_0 by monitoring vibrational autoionization signal. It was found that one autoionizing Rydberg series ($n=15-33$) with the quantum defect of $-0.08--0.10$ (or 0.90–0.92) appears in the transitions from the S_1 vibronic levels accompanied by nontotally symmetric vibrations. According to the symmetry consideration, the Rydberg series should be gerade, and it was tentatively assigned to the *s* Rydberg series.

[a]Authors to whom correspondence should be addressed.

In the present study, we perform similar two-color excitation of autoionizing Rydberg states of the pyrazine–Ar and –Xe clusters via various S_1 vibronic levels, and compare observed spectra with those of bare pyrazine. The spectral shift of the Rydberg series and the appearance of a new Rydberg series tell us the change in the quasi-Coulomb field of the ion core induced by the cluster formation. The competition between the vibrational autoionization and vibrational predissociation of the clusters is discussed based on the autoionization intensity measurements.

II. EXPERIMENT

The experimental apparatus consisted of two laser beam sources and a vacuum chamber. Two dye lasers were simultaneously pumped by a pulsed Nd:YAG laser; the output of a dye laser (DCM dye) was frequency doubled by a KDP crystal and was used to excite pyrazine to the S_1 vibronic level. The second harmonic of the output of another dye laser (Coumarin-460 dye) was used to probe the transitions from the S_1 vibronic level to high Rydberg states. The typical laser pulse energies were 100 and 50 μJ, respectively. Both the laser beams had a spectral resolution of typically 0.5 cm^{-1}, and their pulse duration was 5 ns. Two laser beams were coaxially focused by a lens of $f=500$ mm and were introduced into the interaction region of the vacuum chamber. There was no delay time between the pump and probe laser pulses.

The sample of pyrazine was purchased from Tokyo Kasei Co., and was used without further purification. The sample vapor at room temperature was mixed with pure Ar gas or a gaseous mixture (Xe of 10% in Ar), and was expanded into the vacuum chamber through a pulsed jet nozzle. The stagnation pressure of the carrier gas was 3 bars, and a typical pressure in the chamber was 8×10^{-6} torr during the nozzle operation. The jet expansion was skimmed by a skimmer of 1.5 mm diameter, and the resulting molecular beam was introduced into the interaction region. The produced ions were extracted by a pulsed electric field of 15 V/cm with a voltage increment rate of 3 V/ns into a Wiley–McLaren-type time-of-flight mass spectrometer,[18] and were detected by a channel multiplier. The delay time of 200 ns was arranged between the laser pulses and the pulsed extraction electric field. The ion current was amplified by a preamplifier, and integrated by a gated digital boxcar. The averaged signal was recorded by a personal computer.

III. RESULTS AND DISCUSSION

A. The S_1-S_0 spectra of pyrazine and its rare gas clusters

Figure 1 shows the S_1-S_0 multiphoton ionization (MPI) spectra of jet-cooled (a) bare pyrazine, (b) pyrazine–Ar, and (c) pyrazine–Xe clusters. Each of them was recorded by monitoring the parent cation intensity ($m/e=80$, 120, and 211 amu for bare pyrazine, pyrazine–Ar, and pyrazine–Xe, respectively) as a function of the S_1-S_0 excitation laser wavelength. In pyrazine and its van der Waals clusters, two photon energy of the S_1-S_0 resonant photon is lower than their ionization potentials.[17,19,20] Therefore, another laser

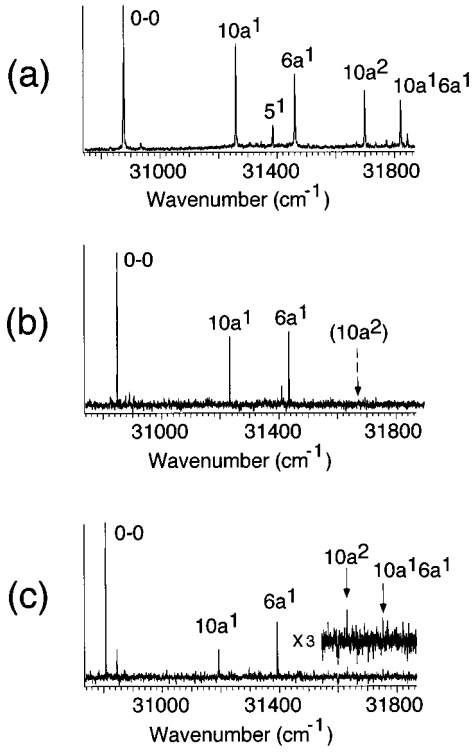

FIG. 1. Multiphoton ionization spectra of the S_1-S_0 transitions of jet-cooled (a) bare pyrazine, (b) pyrazine–Ar, and (c) pyrazine–Xe. Each spectrum was measured by monitoring the parent cation produced by ionization assisted with the laser light of (a) 225 nm, (b) 227 nm, and (c) 227 nm, respectively.

light (225, 227, and 227 nm for bare pyrazine, pyrazine–Ar, and pyrazine–Xe, respectively) was used to assist the ionization from the S_1 state. The intensity of the assist laser was weak enough to avoid two-photon ionization by the assist laser light itself.

The S_1-S_0 spectrum of pyrazine has been extensively studied by many workers,[21] and it is well known that S_1 ($^1B_{3u}$) is due to the (n,π^*) excitation. In the bare molecule, the origin band appears at 30 876 cm^{-1}, and the $10a$ (b_{1g},383 cm^{-1}) and $6a$ (a_g,583 cm^{-1}) vibrations form the major vibronic structure in the low vibrational energy region. The $16b^2$ band ($b_{3u}\otimes b_{3u}$,467 cm^{-1}) disappears in the MPI spectrum while it is seen in the region between the $10a^1$ and the 5^1 (b_{2g},517 cm^{-1}) bands in the absorption spectrum. The disappearance of this band is due to much higher vertical ionization potential from the $16b^2$ level, being compared with that from others.[17,19,20]

The origin band of the pyrazine–Ar cluster was already reported, and is low-frequency shifted by 27 cm^{-1} from that of the bare molecule.[22,23] Several intermolecular vibration bands are seen in the high frequency side of the origin (+27, +41, and +55 cm^{-1}), though their intensities are quite weak. The observed frequencies of the intramolecular vibronic bands of pyrazine–Ar are tabulated in Table I. The $10a$ and $6a$ modes show no changes in their vibrational frequencies upon the cluster formation, and it indicates a weak interaction between pyrazine and Ar. Vibronic bands higher than the $6a^1$ band completely disappear in the spectrum of the cluster obtained by monitoring the parent cation intensity.

TABLE I. Band origins of the S_1-S_0 transition of bare pyrazine, pyrazine–Ar, and pyrazine–Xe with the vibrational frequencies in the S_1 state. All values in cm^{-1}.

	Bare pyrazine[a]	Pyrazine–Ar	Pyrazine–Xe
Band origin[b]	30 876	30 849	30 809
	(0)	(−27)	(−67)
$10a^1$	383	383	384
$6a^1$	583	584	584
$10a^2$	823	822	822
$10a^16a^1$	945		943

[a]From Refs. 17 and 27.
[b]Values in parentheses show relative shifts from the bare molecule.

However, by monitoring the bare cation, a small peak is found at $+822$ cm^{-1} from the origin of pyrazine–Ar [the peak is so weak that it cannot be seen in Fig. 1(a)]. Since the vibrational frequency of $10a^2$ is 823 cm^{-1} in bare pyrazine, the peak at $0_0^0+822\,cm^{-1}$ is assigned to the $10a^2$ band of the cluster. The disappearance of the $10a^2$ band in the cluster spectrum is attributed to the dissociation of the cluster following the ionization, as described in later (see Sec. III E 1).

The structure of pyrazine–Ar has not yet been determined. The structure of pyrimidine–Ar, which is expected to be very similar to that of pyrazine–Ar, was studied by the high resolution rotational structure analysis, and it was confirmed that the Ar atom lies nearly above the center of the pyrimidine ring plane.[24] Moreover, in all aromatic rare gas (1:1) clusters of which structures have been determined so far, it is shown that the Ar atom places on the aromatic ring.[25] Therefore, it is reasonably expected that pyrazine–Ar also has such an out-of-plane structure.

The S_1-S_0 spectrum of pyrazine–Xe is very similar to that of the Ar cluster, showing its origin at 30 809 cm^{-1}. The low-frequency shift of the origin is 67 cm^{-1}, reflecting the higher stabilization energy of this cluster. In the case of the Xe cluster, the $10a^2$ ($+822\,cm^{-1}$) and $10a^16a^1$ ($+943\,cm^{-1}$) bands can be observed by monitoring the parent cluster cation. This fact reflects the higher binding energy of the Xe cluster cation than that of the Ar cluster cation, and the dissociation following the ionization is energetically prohibited. The intensity of the $10a^2$ and $10a^16a^1$ band relative to the origin band is remarkably weaker than that in the bare molecule. This might be attributed to intersystem crossing and vibrational predissociation in the S_1 state, of which rates are known to increase with the cluster formation.[22] The vibrational energies of the Xe cluster in the S_1 state are also tabulated in Table I. As is seen in the Ar cluster, pyrazine–Xe also shows the same vibrational frequencies as the bare molecule. The out-of-plane structure is reasonably expected also for pyrazine–Xe. Intermolecular vibration bands are seen near the origin band ($+39$ and $+65$ cm^{-1}), and their weak intensities indicate small structural change of the cluster upon the electronic excitation.

B. Two-color excitation of high Rydberg series of the bare molecule

The high Rydberg states of bare pyrazine have been studied in the two-color ionization experiments performed by Goto *et al.*[17] We repeated the same experiments as Goto *et al.*, and confirmed their results. In this subsection, prior to present the results on the clusters, we briefly summarize the experiments on bare pyrazine.

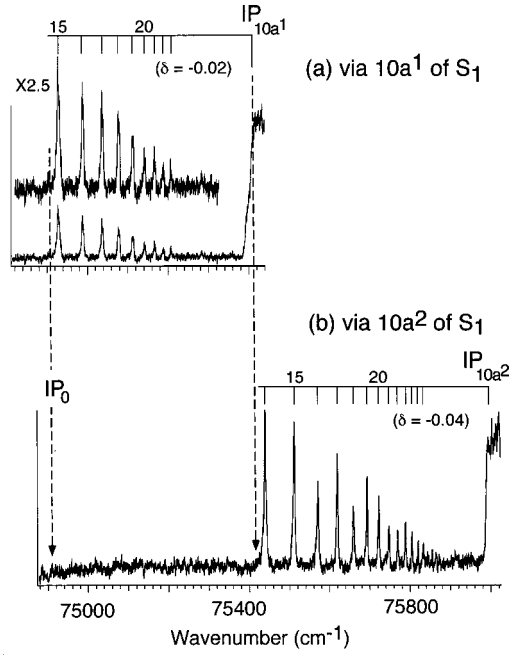

FIG. 2. Two-color ionization spectra of bare pyrazine via the S_1 (a) $10a^1$ and (b) $10a^2$ levels. The converging limits of the Rydberg series are shown by IP_{10a^1} and IP_{10a^2}, respectively.

Figure 2(a) shows the two-color MPI spectrum of jet-cooled bare pyrazine via the $10a^1$ level of the S_1 state. In this spectrum, the frequency of the pumping laser light was fixed to excite the molecule to the S_1 $10a^1$ level while that of the probing laser light was scanned. A Rydberg series starts to appear just above the first ionization threshold (IP_0), and converges to the vertical ionization limit (the $10a^1$ level of the cation: IP_{10a^1}). The disappearance of the Rydberg states lying below IP_0 indicates that the Rydberg series ionizes through the vibrational autoionization.

The term values of the Rydberg series are reproduced by the well-known Rydberg formula,[26]

$$E_n = IP_v - Ry/(n-\delta)^2,$$

where IP_v is the converging limit, Ry is the Rydberg constant (109 736.6 cm^{-1} for bare pyrazine), n is the principal quantum number, and δ is the quantum defect. We carefully calibrated the probing laser frequency by optogalvano spectroscopy with a Ne hollow cathode lamp, and took the S_1-S_0 excitation energy of pyrazine from the report by Udagawa *et al.*[27] Fitting the data by using the above formula, we obtained the averaged quantum defect $\delta=-0.02\pm0.01$ (or $1-0.02=0.98$) and converging limit $IP_{10a^1}=75\,416\pm1.0\,cm^{-1}$. The Rydberg states in the range of $n=15$–23 (or $n=16$–24) were observed.

Goto *et al.* have obtained $IP_{10a^1}=75\,424\,cm^{-1}$ and $\delta=-0.08\pm0.01$ for the same Rydberg series, both of which are slightly different from those obtained in the present measurement.[17] Because of the field ionization effect by the electric field used to extract the ions, it is difficult to directly

measure the vertical ionization threshold. However, zero kinetic energy photoelectron spectroscopy (ZEKE–PES) of pyrazine has been performed by Zhu and Johnson,[20] and IP_0 (74 908 cm^{-1}) and precise vibrational frequencies (502 cm^{-1} for $10a^1$) of the cation have been given (as for the former value, a small low-frequency shift due to the electron extraction field might be involved). When we take our new value of IP_{10a^1} and the vibrational frequency of $10a^1$ given by the ZEKE–PES study, the estimated value of IP_0 results in 74 914 cm^{-1}. This value is consistent with the result of the ZEKE–PES study if the correction due to the ionization field and an experimental uncertainty in the frequency calibration are considered. Therefore, we concluded that the present values are more reliable than old ones given by Goto *et al.*

A pyrazine molecule belongs to the D_{2h} point group, and the symmetry of the intermediate S_1 $10a^1$ level is $B_{3u}\otimes b_{1g}=B_{2u}$. The Rydberg states created by the dipole allowed transitions from the S_1 $10a^1$ level must have the gerade symmetry because the photon carries the ungerade symmetry. For such gerade Rydberg states, two cases are possible with respect to the symmetry; one is the case that both the ion core and the Rydberg electron have the gerade symmetry, and the other is that both have the ungerade symmetry. For pyrazine cation, the electronic ground state (D_0) is expected to be of ^2A_g, because a nonbonding electron of the a_g symmetry is ejected upon the ionization.[17] Assuming the same D_{2h} point group for the cationic state, the Rydberg series converging to IP_{10a^1} must have the gerade ion core of $^2A_g\otimes b_{1g}=^2B_{1g}$. Thus, the Rydberg electron should be of gerade.

It has been known that Rydberg states with high orbital angular momentum ($l\geqslant 4$, i.e., $g,h,i,\ldots$) are rarely found in transitions from a valence state because of a poor overlap between electronic wave functions.[4,28] In this respect, we expect that $s\,(l=0)$ or $d(l=2)$ Rydberg series are the most probable candidates for the observed Rydberg series. Typical quantum defects of s and d Rydberg series are ≈ 1 and ≈ 0.1, respectively, and it is also known that the d Rydberg series sometimes has a negative value for the quantum defect because of the interaction with the s Rydberg series.[28] Since $(n+1)s$ and nd Rydberg series occur in the similar term energies, it is hard to distinguish these two Rydberg series by the observed band positions. In fact, the observed quantum defect, $\delta=-0.02$ (or $1-0.02=0.98$) is consistent with both of the candidates. Goto *et al.* have tentatively assigned the observed series to the s Rydberg series.[17] In the rest of this paper, we tentatively use the negative value of δ (-0.02). This is simply for convenience, because it enables us to use the same principal quantum number for the Rydberg state which is newly found in the clusters as described in the latter section [see Sec. III C 1]. As for the assignment of this gerade Rydberg series, we also emphasize that the definitive conclusion cannot be given at the present stage.

The same Rydberg series with the different vibrational state of the ion core is also observed in the two-color MPI spectrum via the S_1 $10a^2$ level of bare pyrazine, as shown in Fig. 2(b). A Rydberg series appears to converge to the vertical ionization threshold ($IP_{10a^2}=75\,997\ cm^{-1}$). The $10a^2$ vibrational frequency in the cation is evaluated to be 1083 cm^{-1} when we take $IP_0=74\,914\ cm^{-1}$. This value is consistent with that given by the ZEKE–PES work by Zhu and Johnson (1086 cm^{-1}).[20] The quantum defect of the $10a^2$ Rydberg series is estimated to be -0.04 (± 0.01), and it is slightly shifted with the vibrational excitation of the ion core. The previous measurement by Goto *et al.* reported $IP_{10a^2}=75\,995\ cm^{-1}$ and $\delta=-0.09$.[17] The differences from the present measurement are much smaller than those of the $10a^1$ Rydberg series.

The $10a^2$ Rydberg series is not observed below the IP_{10a^1} threshold (75 416 cm^{-1}). This fact shows that the well-known $\Delta v=-1$ propensity rule for vibrational autoionization is held even in a large polyatomic molecule.[26,29] It is also worth to note that the vertical transitions ($\Delta v=0$) are strongly favored from the $10a^1$ and $10a^2$ levels of the S_1 state. No direct ionization to the $\Delta v=-1$ continuum occurs, and it enables us to observe the autoionizing Rydberg series without the interference from the direct ion. Goto *et al.* showed that such an exclusive preference of vertical transitions is only found in the transitions from the S_1 vibronic levels involving the nontotally symmetric vibrations such as the $10a\,(b_{1g})$ mode.[17] The levels containing totally symmetric vibrations such as the $6a(a_g)$ mode show strong direct ionization of $\Delta v=-1$, leading to the destructive interference with the transitions to the Rydberg states (see Sec. III D).

Comparing the spectra of the $10a^1$ and $10a^2$ Rydberg series, it is seen that the intensity of the autoionization signal relative to the direct ionization intensity at IP_v is quite different. The Rydberg series of the $10a^2$ ion core shows much stronger autoionization intensity. If the autoionization efficiency of the Rydberg series is unity, the intensity of the Rydberg series smoothly converges to the direct ionization intensity, and no step structure appears at the converging limit.[30,31] The appearance of the step structure at the direct ionization threshold indicates the presence of the competing decay processes such as electronic predissociation. The observed autoionization intensities relative to the direct ionization reflect the larger autoionization efficiency of the $10a^2$ ion core than the $10a^1$ ion core.

C. High Rydberg states of the clusters with the $10a^1$ ion core

1. Pyrazine–Ar

Shown in Fig. 3(a) is the two-color MPI spectrum via the S_1 $10a^1$ level of pyrazine–Ar. The gross feature of the spectrum is very similar to that of the bare molecule; autoionizing Rydberg series appear in the region between IP_0 and IP_{10a^1}, and the direct ionization to the continuum of $v=0$ does not occur. However, two Rydberg series are seen in the spectrum of the cluster, while only one series appears in the corresponding spectrum of the bare molecule. The intensity of the dominant Rydberg series is about double of that of the weaker series. The term values of both the Rydberg series are well fitted by the Rydberg formula, and the resulting converging limit and quantum defects are tabulated in Table II. It was found that both the Rydberg series converge to the same limit (75 132 cm^{-1}), indicating that these two Rydberg series have the same $10a^1$ ion core. The quantum defect of

TABLE II. Averaged quantum defects and converging limits of the Rydberg series of the $10a^1$ ion core.

	Quantum defect[a]		Converging limit/ cm^{-1} [b]	First ionization threshold/cm^{-1} [c]
Bare pyrazine	−0.02		75 416	74 914
Pyrazine–Ar	−0.09	+0.04	75 132	74 630
Pyrazine–Xe	−0.13	+0.02	74 909	74 407

[a]The estimated error is ±0.01.
[b]The estimated error is ±1 cm^{-1}.
[c]Converging limit −502 (the $10a^1$ vibrational frequency of the bare cation) cm^{-1}.

the dominant series is very small and negative ($\delta=-0.09$), and it is similar to that of the bare molecule ($\delta=-0.02$). On the other hand, the quantum defect of the weaker series is positive, but its absolute values is also very small ($\delta=0.04$). By using these values, the first ionization threshold of pyrazine–Ar is found to be 74 630 cm^{-1}, if we adapt the same $10a^1$ vibrational frequency of the cluster cation as that of the bare cation (502 cm^{-1}), which is reasonable with respect to its out-of-plane structure.

2. Pyrazine–Xe

The two-color MPI spectrum via the $S_1\ 10a^1$ level of pyrazine–Xe is shown in Fig. 3(b). The spectrum is quite similar to that of pyrazine–Ar. Two autoionizing Rydberg series are seen in the spectrum, and both of them converge to the same vertical ionization threshold (IP_{10a^1}). The averaged quantum defects of the Rydberg series are tabulated in Table II. They are very similar to those of pyrazine–Ar, but show larger shifts to the negative direction.

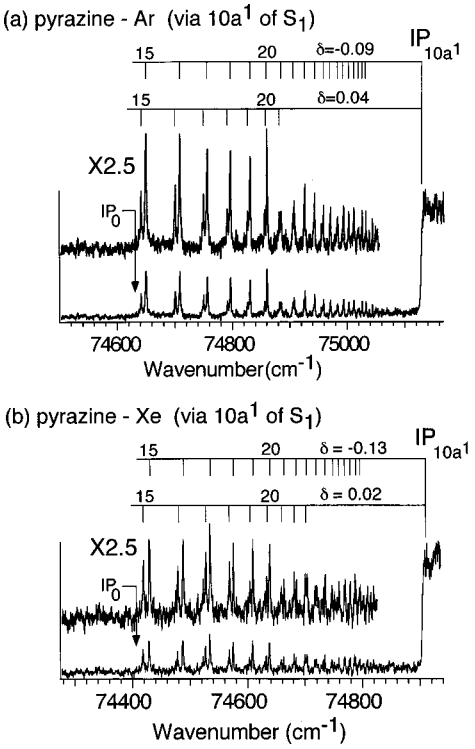

FIG. 3. Two-color ionization spectra of (a) pyrazine–Ar and (b) pyrazine–Xe via the $S_1\ 10a^1$ level.

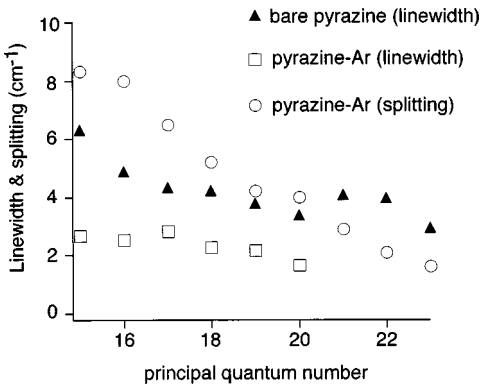

FIG. 4. Principal quantum number dependence of the linewidths of the Rydberg series of bare pyrazine and pyrazine–Ar (the dominant series) together with the dependence of the splittings between the two Rydberg series of pyrazine–Ar (see text).

Moreover, it is found that the intensity of the weaker series relative to the dominant series is much stronger in pyrazine–Xe. The intensity of the weaker series is roughly 2/3 of that of the dominant series.

Since the converging limit of the $10a^1$ Rydberg series of pyrazine–Xe is found to be 74 909 cm^{-1}, the first ionization threshold is estimated to be 74 407 cm^{-1}, when we adapt the same $10a^1$ frequency (502 cm^{-1}) as the bare cation.

3. Assignment of the Rydberg series: symmetry breakdown of the ion core by the cluster formation

Both in the spectra of the pyrazine–Ar and –Xe clusters, the two Rydberg series of the $10a^1$ ion core appear while only one series is seen in the corresponding spectrum of bare pyrazine. The quantum defects of the dominant series in the clusters are similar to that of the gerade Rydberg series of the bare molecule, and the relative intensities to the step structure at the direct ionization threshold are also similar to. Therefore, it is reasonably concluded that they are attributed to the same gerade (*d* or *s*) Rydberg series as that found in bare pyrazine.

For the assignment of the weaker Rydberg series observed only in the clusters, there are two possibilities; (a) the m_l splitting of the orbital angular momentum (l) of the Rydberg electron originating from the enhanced anisotropy of the solvated ion core (in this case, l should be *d* or higher). (b) An ungerade (*f* or higher ungerade) Rydberg series, which is forbidden in the D_{2h} bare molecule, appears in the clusters because of the breakdown of the ion core symmetry.

Several hints to examine the above possibilities are provided in the observed spectra as follows.

(i) Though the m_l splitting is expected to occur even in the bare molecule because of the nonspherical field of the ion core, there is no sign of such splitting in the bare molecule. This is confirmed by Fig. 4 which shows the n dependence of the linewidths (full width at half maximum) of the Rydberg series of bare pyrazine and of pyrazine–Ar (the dominant series), together with the n dependence of the splittings between the two Rydberg series of pyrazine–Ar. The linewidths were evaluated by the Lorentzian line shape fitting.

We neglected deconvolution procedure of the laser linewidth (lower than 0.3 cm^{-1} in the linewidth measurement experiments). This is because the linewidths of the Rydberg series are much broader than the laser linewidth and the uncertainty due to the fluctuation of the observed band shape is as large as the laser linewidth. Total uncertainty of the linewidths was estimated to be 0.5 cm^{-1}. Though n^{-3} dependence is generally expected for linewidths of Rydberg series,[26] the observed linewidths are almost constant for both the bare molecule and cluster. This indicates that the observed linewidths are mainly attributed to the rotational contour but are not governed by the lifetimes of the Rydberg states. The linewidths of the bare molecule are wider than those of the cluster, however, the wider linewidths cannot be attributed to unresolved splitting of the Rydberg series in the bare molecule. If the linewidths of the bare molecule arise from the unresolved splittings of the Rydberg series, the linewidths should show strong n dependence as the splittings of the cluster. The narrower linewidths of the cluster are attributed to the decrease of the rotational constant associated with the cluster formation.

(ii) Since the polarizabilities of Ar and Xe are 1.641×10^{-24} and $4.044\times10^{-24}\,cm^3$, respectively,[32] much larger splitting of the two series is expected for pyrazine–Xe than pyrazine–Ar, if the extra Rydberg series arises from the splitting of the m_l components. As seen in the quantum defects in Table II, however, the splittings of the two Rydberg series, which are represented by the quantum defect difference between the two series, are almost the same for both the pyrazine–Ar and –Xe clusters.

(iii) In pyrazine–Xe, the intensity of the weaker Rydberg series relative to the dominant series is larger than that in pyrazine–Ar.

The hints (i) and (ii) are not in accord with the possibility (a), the m_l splitting, while the hints (i)–(iii) are consistent with the possibility (b), the symmetry breakdown of the ion core. Therefore, all the characteristics of the extra series represent that the possibility (b) seems to be more likely than the possibility (a). The small quantum defect of the Rydberg series indicates that the orbital angular momentum of the Rydberg electron should be higher than $l=1$, and we tentatively assign the weaker Rydberg series in the clusters to the f $(l=3)$ Rydberg series.

4. Autoionization efficiency of the $10a^1$ Rydberg states of the clusters

By monitoring the cluster cation intensity, the direct ionization to the $10a^1$ continuum is clearly observed both for pyrazine–Ar and pyrazine–Xe. This means that the $10a^1$ level of both the cluster cations $(+502\ cm^{-1})$ is lower than their dissociation threshold, and no vibrational predissociation takes place for both the vibrationally excited ion core.

Below the dissociation threshold of the van der Waals bond, the dynamics of the Rydberg cluster lying above IP_0 is characterized by the competition between the vibrational autoionization and the *electronic* predissociation.[12–14] It is found by the comparison of Figs. 2 and 3 that the relative intensities of the gerade (dominant) Rydberg transitions versus the direct ionization to the $10a^1$ continuum are almost the same among the bare molecule and the clusters. Since the direct ionization efficiency is expected not to be affected by the cluster formation, it is concluded that the autoionization (and also electronic predissociation) efficiency of the clusters is left unchanged as that of the bare molecule.

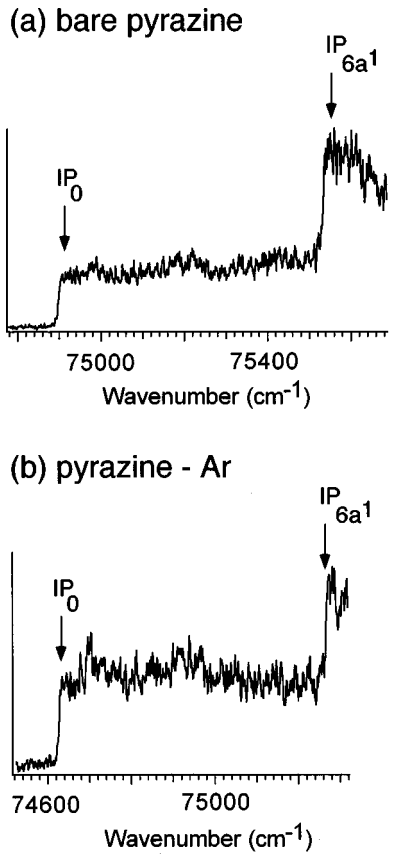

FIG. 5. Two-color ionization spectra of (a) bare pyrazine and (b) pyrazine–Ar via the $S_1\,6a^1$ level. The adiabatic and vertical ionization thresholds are shown by IP_0 and IP_{6a^1}, respectively.

D. Two-color ionization via the $S_1\,6a^1$ level

Figure 5(a) shows the two-color ionization spectrum of bare pyrazine via the $S_1\,6a^1\,(a_g)$ level $(+583\ cm^{-1})$. As already found by Goto *et al.*, no Rydberg series is seen in the transition from the S_1 vibronic level containing the totally symmetric vibration such as the $6a$ mode, while the remarkable step structures appear at the ionization thresholds with respect to the $v=0$ and 1 continua.[17]

The corresponding two-color ionization spectrum of pyrazine–Ar is shown in Fig. 5(b), obtained by monitoring the cluster cation intensity. The spectrum of the cluster is quite similar to that of the bare molecule, exhibiting the step structures at the direct ionization thresholds for $v=0$ and the $6a^1$ continua. Since the vibrational frequency of the $6a$ mode of the bare pyrazine cation has been precisely determined to be 632 cm^{-1} by ZEKE spectroscopy,[20] it is reasonable to assume the same vibrational frequency for the pyrazine–Ar cation. Therefore, the appearance of the step structure at the direct ionization to the $6a^1$ continuum indicates that the dissociation threshold of the pyrazine–Ar cation is higher than 632 cm^{-1}.

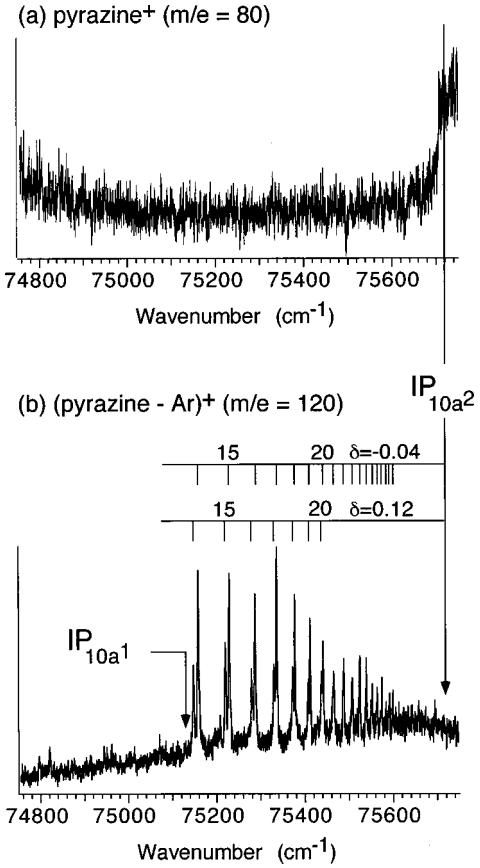

FIG. 6. Two-color ionization spectra of pyrazine–Ar via the $S_1\ 10a^2$ level. The spectra were measured by monitoring (a) the bare pyrazine cation and (b) the cluster cation.

E. High Rydberg states in the clusters with the $10a^2$ ion core

1. Pyrazine–Ar

Shown in Fig. 6 are the two-color MPI spectra of pyrazine–Ar via the $S_1\ 10a^2$ level obtained by monitoring (a) the bare molecular cation ($m/e=80$ amu) and (b) the cluster cation ($m/e=120$ amu). In the spectrum (b), two Rydberg series are seen, converging to the vertical ionization threshold (the $10a^2$ level of the cation). The Rydberg series are quite similar to those found in the transitions via the $S_1\ 10a^1$ level, and they are clearly assigned to the gerade (s or d) and ungerade (f) Rydberg series of the $10a^2$ ion core. Their converging limit and quantum defects are tabulated in Table III. The $10a^2$ vibrational energy of the cluster cation is estimated to be 1084 cm^{-1} from the difference between the first ionization threshold and the converging limit. This value is almost the same as that of the bare cation (1083 cm^{-1}) estimated by the same method. As seen in the corresponding spectrum of bare pyrazine [Fig. 2(b)], only the Rydberg states lying above the $10a^1$ threshold (IP_{10a^1}) appear in the spectrum, indicating that the vibrational autoionization propensity rule of $\Delta v=-1$ is held also in the cluster.[26,29]

TABLE III. Averaged quantum defects and converging limits of the Rydberg series of the $10a^2$ ion core.

	Quantum defect[a]		Converging limit/ cm^{-1} [b]
Bare pyrazine	−0.04		75 997
Pyrazine–Ar	−0.04	+0.12	75 715
Pyrazine–Xe	−0.11	+0.05	75 488

[a]The estimated error is ±0.01.
[b]The estimated error is ±1 cm^{-1}.

A remarkable feature of the spectrum (b) of the cluster is the disappearance of the step structure at the direct ionization threshold (IP_{10a^2}). On the other hand, the spectrum (a), obtained by monitoring the bare cation, shows a clear step at the direct ionization threshold, while no Rydberg series is seen.

The characteristic features of the cluster spectra indicate that the $10a^2$ level of the cluster cation lies above the dissociation threshold of the van der Waals bond. When the cluster is directly ionized into the $10a^2$ ionization continuum, there is no way to release the vibrational energy except for the vibrational predissociation, and all the cluster cations finally dissociate into the bare cation. Thus, the step structure due to the direct ionization is seen only in the spectrum (a), but it disappears in the spectrum (b). On the other hand, the Rydberg series of the $10a^2$ ion core can release the vibrational energy through the vibrational autoionization. In the vibrational autoionization process, the ion core looses one quanta of its vibrational energy to eject the Rydberg electron.[26,29] The cluster ion results in the $10a^1$ level which lies below the dissociation threshold, as described in Sec. III C 4. Thus, the Rydberg states lying above the dissociation threshold appear in the spectrum (b), if the vibrational autoionization is faster than the vibrational predissociation of the ion core.

2. Competition between the vibrational autoionization and vibrational predissociation

As described in Sec. III D, the dissociation threshold of the pyrazine–Ar cation should be higher than the $6a^1$ level (+632 cm^{-1}). The $6a^1$ level of the cluster cation lies at +75 262 cm^{-1} from the zero vibrational level of S_0, and this energy level ($IP_0+632\ cm^{-1}$) falls in the region between $n=15$ and 16 of the $10a^2$ Rydberg states of the cluster. On the other hand, the upper limit of the dissociation threshold of the cluster cation is given by the recent infrared dissociation spectroscopic study.[33] Remmers *et al.* measured infrared spectrum of pyrazine–Ar in the lowest triplet state (T_1) by monitoring the vibrational predissociation of the cluster. The lowest vibrational frequency they observed was 510 cm^{-1}, which represents an upper limit of the dissociation energy of the cluster in the T_1 state. Upon the cluster formation with Ar, it has been shown the low-frequency shift of the T_1-S_0 transition is 16 cm^{-1},[34] and the adiabatic ionization threshold is 284 cm^{-1}. By using these values, the upper limit of the binding energy of the pyrazine–Ar cation is evaluated to be 778 cm^{-1}. This upper limit lies at +75 408 cm^{-1} ($IP_0+778\ cm^{-1}$) from the zero vibrational level of S_0, and just falls on $n=19$ of the $10a^2$ Rydberg states of the cluster.

In the Rydberg states of the cluster lying just above the dissociation threshold of the cluster cation, the vibrational autoionization is expected to compete with the vibrational

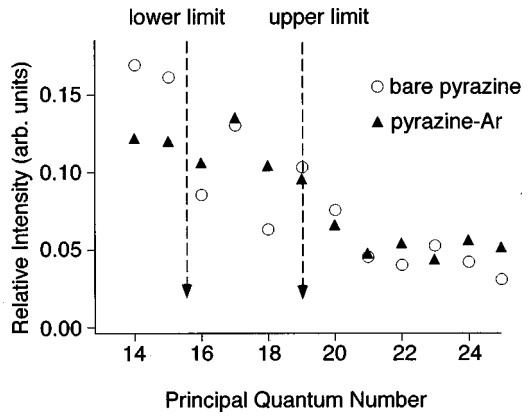

FIG. 7. Intensity distributions of the $10a^2$ Rydberg series of bare pyrazine and pyrazine–Ar (the dominant series) observed in the two-color ionization spectra shown in Fig. 2(b) and Fig. 6(b), respectively. Each mark represents the peak intensity of the Rydberg transition normalized by the sum of the peak intensities of the Rydberg transitions from $n=14$ to 25. The arrows indicate the lower and upper limits of the dissociation threshold of the van der Waals bond in the ion core of the cluster (see text).

predissociation (of the ion core). When the vibrational predissociation occurs prior to the autoionization, the ion core releases its all the vibrational energy, resulting in high Rydberg states of the bare molecule lying below the first ionization threshold. Thus, if the predissociation is dominant over the autoionization, a sudden decrease of the autoionization efficiency should be found just above the dissociation threshold.

Figure 7 shows the intensity distributions of the $10a^2$ autoionizing Rydberg series of bare pyrazine and of corresponding pyrazine–Ar. In this figure, each mark represents the peak intensity normalized by the sum of the peak intensities of all the Rydberg transitions from $n=14$ to 25. In the case of pyrazine–Ar, the dissociation threshold of the van der Waals bond is in the region of $15<n\leqslant 19$, and the vibrational predissociation may compete with the vibrational autoionization above this region, leading to an intensity reduction. However, the intensity distribution of the Rydberg series in the cluster is almost the same as that of the bare molecule, indicating no sign of the competition of the vibrational predissociation vs the vibrational autoionization. Thus, it is concluded that the vibrational autoionization rate is much faster than the vibrational predissociation rate, and the autoionization efficiency is not affected by the opening of the dissociation channel.

3. Pyrazine–Xe

The two-color ionization spectrum of pyrazine–Xe via the $S_1\ 10a^2$ level is shown in Fig. 8. Though the spectrum was recorded by monitoring the cluster cation intensity, a clear step structure appeared at the direct ionization threshold to the $10a^2$ continuum. This fact means that the dissociation threshold of the pyrazine–Xe cation lies above the $10a^2$ level, and is much higher than that of the pyrazine–Ar cation. The larger van der Waals binding energy of the pyrazine–Xe cation is consistent with the much larger polalizability of Xe than that of Ar.

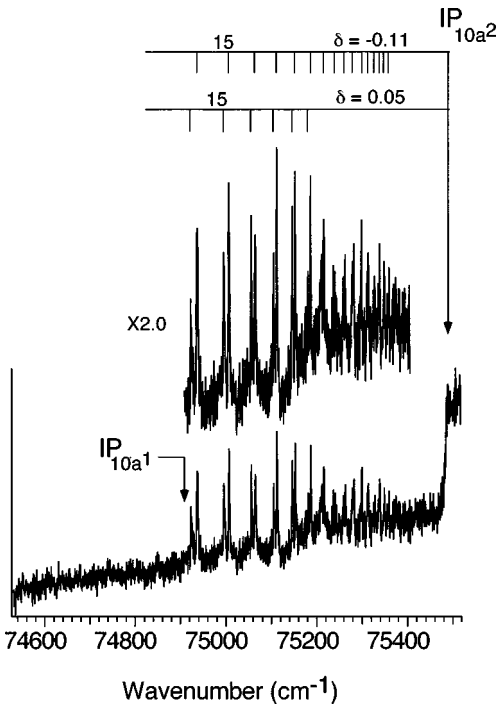

FIG. 8. Two-color ionization spectrum of pyrazine–Xe via the $S_1\ 10a^2$ level measured by monitoring the cluster cation.

Two autoionizing Rydberg series converging to the $10a^2$ level of the cluster cation appear also in the case of pyrazine–Xe. The converging limit and quantum defects evaluated from the spectrum are summarized in Table III. The $10a^2$ vibrational frequency of the cluster cation is estimated to be 1081 cm^{-1} from the difference between the adiabatic and $10a^2$ ionization thresholds. This value is almost the same as those of the bare and the Ar cluster cations. The quantum defects of the Rydberg series are slightly shifted to the negative direction comparing with those of pyrazine–Ar. The dominant and weaker Rydberg series are attributed to the gerade (s or d) and ungerade (f) Rydberg series, respectively, and the latter series is seen only in the cluster because of the symmetry restriction. As seen in the $10a^1$ Rydberg series, the intensity of the ungerade series relative to the gerade series is larger than that in the pyrazine–Ar spectrum, suggesting the more extensive breakdown of the D_{2h} symmetry in pyrazine–Xe.

The intensity of the Rydberg series relative to the direct ionization at the $10a^2$ threshold is almost the same as that of the bare molecule. Therefore, it is concluded that the cluster formation does not affect on the autoionization efficiency, as seen in the $10a^1$ Rydberg states.

F. Quantum defect change due to the cluster formation

In Rydberg states having such a high n as we observed in this study, the orbital radius of the Rydberg electron is much larger than the size of the ion core, so that an influence on the electron by the ion core is expected not to be so effective. Though the Rydberg electron is mostly in the region far away from the ion core, it sometimes closes to the ion core, and strongly interacts with the nonspherical field

near the ion core. Such phenomenon is called core penetration, and it causes a quantum defect of the Rydberg series.[12] In the case of the Rydberg states of the pyrazine clusters, it is expected that the solvent atom partly prevents the Rydberg electron from the core penetration into the pyrazine moiety, in which the positive charge is localized. This effect reduces the binding energy of the Rydberg electron, resulting in the shift of the quantum defect to the negative direction.

In this study, we observed the $10a^1$ and $10a^2$ Rydberg series of pyrazine–Ar and –Xe. Their quantum defects are summarized in Tables II and III, together with those of the bare molecule. As we expected above, it is evident that the quantum defects of the Rydberg series tend to shift to the negative direction upon the cluster formation, except for the case of the $10a^2$ Rydberg series of pyrazine–Ar. Moreover, the shifts are larger in pyrazine–Xe than pyrazine–Ar, reflecting the larger size of the atom, i.e., the larger shielding effect. Of course, it should be noted that the above discussion is quite qualitative, and more complicated factors may contribute to the quantum defect, as seen in the exceptional behavior of the gerade $10a^2$ Rydberg series of pyrazine–Ar.

IV. SUMMARY

In this paper, we studied spectroscopy and dynamics of the autoionizing Rydberg states in the pyrazine–Ar and –Xe clusters. The autoionization spectra of the clusters were compared with those of the bare molecule, and the solvation effects on the ion core of the high Rydberg states were extracted. In addition to the gerade (*s* or *d*) Rydberg series which appears in the spectrum of the bare molecule, a new Rydberg series was found in the clusters. This new Rydberg series was assigned to the ungerade (*f*) Rydberg series which is symmetry forbidden in the bare molecule. It was suggested that the symmetry breakdown of the quasi-Coulomb field of the ion core is induced by the cluster formation. With the cluster formation, the quantum defects of the Rydberg series tend to shift to the negative direction, indicating the reduction of the Rydberg electron binding energy due to the shielding effect of the rare gas atoms. The autoionization efficiency is not remarkably affected by the cluster formation, even above the dissociation threshold of the van der Waals bond. It was concluded that autoionization decay is dominant over the vibrational predissociation in the region just above the dissociation threshold.

ACKNOWLEDGMENTS

The authors greatly acknowledge Professor T. Ebata, Professor H. Kono, and Dr. H. Ishikawa at Tohoku University for stimulated discussion. We are also grateful to Professor Y. Hatano at Kyushu University for helpful suggestions. This work was supported by Matsuo Foundation.

[1] E. Rühl, B. Brutschy, and H. Baumgärtel, Chem. Phys. Lett. **157**, 379 (1989).
[2] D. Bahatt, U. Even, and A. Gedanken, J. Phys. Chem. **97**, 7189 (1993).
[3] Y. Lu *et al.*, Z. Phys. D: At., Mol. Clusters **35**, 125 (1995).
[4] T. M. Di Palma, A. Latini, M. Satta, and A. Giardini-Guidoni, Eur. Phys. J. D **4**, 225 (1998).
[5] K. Siglow, R. Neuhauser, and H. J. Neusser, J. Chem. Phys. **110**, 5589 (1999).
[6] M. Okunishi, K. Yamanouchi, and S. Tsuchiya, J. Chem. Phys. **97**, 2305 (1992); M. Okunishi, K. Yamanouchi, K. Onda, and S. Tsuchiya, *ibid.* **98**, 2675 (1993).
[7] For example, K. Tsuji, K. Shibuya, and K. Obi, J. Chem. Phys. **100**, 5441 (1994), and references therein.
[8] M. C. R. Cockett, J. G. Goode, R. R. J. Maier, K. P. Lawley, and R. J. Donovan, J. Chem. Phys. **101**, 126 (1994).
[9] Q. Y. Shang, P. O. Moreno, S. Li, and E. R. Bernstein, J. Chem. Phys. **98**, 1876 (1993).
[10] Q. Y. Shang, P. O. Moreno, C. Dion, and E. R. Bernstein, J. Chem. Phys. **98**, 6769 (1993).
[11] Q. Y. Shang, C. Dion, and E. R. Bernstein, J. Chem. Phys. **101**, 118 (1994).
[12] H. Nakamura, Int. Rev. Phys. Chem. **10**, 123 (1991).
[13] Y. Hatano, Phys. Rep. **313**, 109 (1999).
[14] A. Fujii and N. Morita, Chem. Phys. Lett. **182**, 304 (1991).
[15] For example, in *Clusters of Atoms and Molecules*, edited by H. Haberland (Springer-Verlag, Berlin, 1993 and 1994), Vols. I and II, and references therein.
[16] J. M. Warman, in *The Study of Fast Processes and Transient Species by Electron Pulse Radiolysis*, edited by J. H. Baxendale and F. Busi (Reidel, Dordrecht, 1982).
[17] A. Goto, M. Fujii, and M. Ito, J. Phys. Chem. **91**, 2268 (1987).
[18] W. C. Wiley and I. H. McLaren, Rev. Sci. Instrum. **26**, 1150 (1955).
[19] S. Hillenbrand, L. Zhu, and P. Johnson, J. Chem. Phys. **95**, 2237 (1991).
[20] L. Zhu and P. Johnson, J. Chem. Phys. **99**, 2322 (1993).
[21] J. Kommandeur, W. A. Majewski, W. L. Meerts, and D. W. Pratt, Annu. Rev. Phys. Chem. **38**, 433 (1987), and references therein.
[22] A. Goto, M. Fujii, N. Mikami, and M. Ito, J. Phys. Chem. **90**, 2370 (1986).
[23] L. M. Yoder, J. R. Barker, K. T. Lorenz, and D. W. Chandler, Chem. Phys. Lett. **302**, 602 (1999).
[24] Y. Sugawara, N. Mikami, and M. Ito, J. Phys. Chem. **90**, 5619 (1986).
[25] For example, Th. Weber, A. von Bargen, E. Riedle, and H. J. Neusser, J. Chem. Phys. **92**, 90 (1990).
[26] H. Lefebvre-Brion and R. W. Field, *Perturbations in the Spectra of Diatomic Molecules* (Academic, Orlando, 1986).
[27] Y. Udagawa, M. Ito, and I. Suzuka, Chem. Phys. **46**, 237 (1980).
[28] M. B. Robin, *Higher Excited States of Polyatomic Molecules* (Academic, New York, 1974), Vol. I.
[29] R. S. Berry, J. Chem. Phys. **45**, 1228 (1966).
[30] S. T. Pratt, J. L. Dehmer, and P. M. Dehmer, J. Chem. Phys. **90**, 2201 (1989).
[31] A. Fujii and N. Morita, J. Chem. Phys. **103**, 6029 (1995).
[32] *CRC Handbook of Chemistry and Physics*, edited by D. R. Lide (CRC, Boca Raton, FL, 1995).
[33] K. Remmers *et al.*, Chem. Phys. Lett. **317**, 197 (2000).
[34] E. Villa, M. Terazima, and E. C. Lim, Chem. Phys. Lett. **129**, 336 (1986).